

Stabilization of Nitrosyls by Surface Oxygen: Structure and Reactivity of NO on Oxygen-Modified Mo(110)

K. T. Queeney[†] and C. M. Friend*

Department of Chemistry, Harvard University, 12 Oxford Street, Cambridge, Massachusetts 02138

Received: May 12, 1998; In Final Form: September 11, 1998

The effects of preadsorbed atomic oxygen on nitric oxide (NO) structure and reactivity on Mo(110) are studied via temperature programmed reaction, high-resolution electron energy loss spectroscopy, and infrared reflectance absorbance spectroscopy. NO reaction on two different oxygen overlayers—a saturated low-temperature surface overlayer and a thin-film oxide—is studied in detail. The dissociation of NO to atomic nitrogen and oxygen, the predominant pathway for NO reaction on clean Mo(110), is inhibited by surface oxygen, even though NO dissociation displaces surface oxygen from high- to low-coordination sites. The same low-temperature pathways observed for N–N bond formation on clean Mo(110)—N₂O formation from dinitrosyl coupling and N₂ formation from reaction of molecular NO with atomic nitrogen—are observed on the oxygen-modified surfaces, but in lesser relative and absolute amounts than on clean Mo(110). As oxygen coverage is increased, NO desorption becomes the dominant reaction pathway and occurs at increasingly higher temperatures. Vibrational spectroscopy is used to correlate desorption features with distinct NO species, which vary qualitatively with oxygen coverage. We find that, in contrast to earlier studies on other oxygen-modified transition metal surfaces, NO desorption temperature cannot be correlated with the strength of the metal–NO interaction as judged by the internal N–O stretch frequency.

Introduction

The reactions of nitric oxide (NO) on transition metal surfaces are of great interest due to the presence of NO and NO_x species as pollutants in both stationary sources and automobile exhaust. Studies have shown that the addition of molybdena (MoO₃) to a variety of noble-metal-containing catalysts enhances their activity for NO reduction.^{1–4} Since NO is known to form dinitrosyls (Mo(NO)₂) on MoO₃,^{5–7,1} it has been proposed¹ that N–N bond formation is enhanced via this coupling of intact NO molecules through a common adsorption site.

Previously, we have shown that NO forms dinitrosyls on Mo(110) upon adsorption at 100 K; these species react to evolve N₂O below 300 K, and unreacted dinitrosyls are stable in ultrahigh vacuum to temperatures as high as 500 K.⁸ Importantly, this is the first single-crystal study to demonstrate metal-mediated coupling of NO molecules en route to N–N bond formation. Condensed-phase type dimers have been identified spectroscopically on Ag(111)^{9,10} and Cu(111)¹¹ at 90 K, above the temperature for NO condensation, but the vibrational spectra of these dimers are virtually unperturbed from those of gas- and condensed-phase (NO)₂ species, indicating minimal interaction of (NO)₂ with the metal surfaces.

On clean Mo(110), NO forms dinitrosyls only after dissociation of ~0.65 ML of NO, suggesting that surface oxidation is required for formation of these catalytically relevant species. Atomic oxygen deposited by NO dissociation was shown to reside in high-coordination and terminal (Mo=O) sites on Mo(110), but it is not known what role, if any, dissociated nitrogen atoms play in inhibiting NO dissociation and stabilizing surface dinitrosyl species.

In the present study we have examined the effect of oxygen atoms in specific coordination sites and at specific coverages on NO adsorption and reactivity on Mo(110). Using well-characterized protocols for preparation of oxygen overlayers,¹² we have examined in some detail the structure and subsequent reactive chemistry of NO both on a Mo(110) surface with oxygen deposited exclusively in high-coordination surface sites and on a thin-film oxide. While oxygen clearly inhibits dissociation of NO on Mo(110), we find no evidence that preoxidation of Mo(110) stabilizes or favors formation of dinitrosyls. To the contrary, increasing the oxygen content of the surface stabilizes monomeric forms of NO to result in NO desorption, the least desired reaction pathway from a pollution-reduction point of view, at progressively higher temperatures.

Experimental Section

Experiments were performed in two separate ultrahigh vacuum chambers which have been described fully elsewhere.^{13,14} Each is equipped with LEED optics, a cylindrical mirror analyzer for Auger electron spectroscopy, and a computer-controlled quadrupole mass spectrometer (UTI 100-C) for monitoring of up to 10 separate masses in a single temperature-programmed reaction experiment.¹⁵ Protocols for sample preparation and cleaning^{16,8} and temperature-programmed reaction experiments⁸ are given elsewhere.

One chamber¹³ houses a high-resolution electron energy loss spectrometer (LK Technologies, model LK-2000); electron energy loss spectra were collected with a primary beam energy of 3 eV and specular detection. The second chamber¹⁴ is interfaced to a Nicolet Series 800 clean-air purged FTIR spectrometer for infrared reflectance absorbance spectroscopy. Infrared spectra were collected with an MCT-A detector at 4 cm⁻¹ resolution unless otherwise noted.¹⁷ Typically, 500 sample

[†] Present address: Bell Laboratories, Lucent Technologies, 700 Mountain Avenue, Murray Hill, NJ 07974.

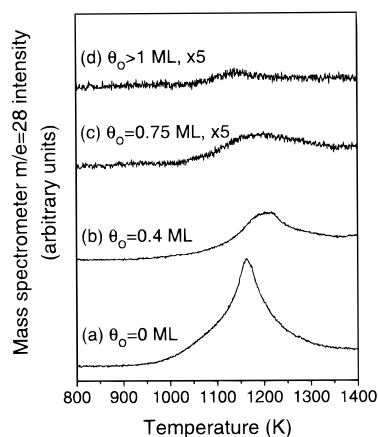


Figure 1. Temperature programmed reaction of recombinant N_2 formation from dissociation of a saturated NO overlayer on (a) clean Mo(110), (b) a surface oxygen overlayer with $\theta_O \approx 0.4$ ML, (c) a surface oxygen overlayer with $\theta_O \approx 0.75$ ML, and (d) a thin-film oxide. Note expanded scale in (c) and (d). Heating was accomplished via electron bombardment, with the sample biased at ~ 100 V; the heating rate was ~ 10 K s^{-1} .

scans were ratioed against a background obtained after flashing the crystal to ~ 750 K and allowing it to return to ~ 100 K.

Oxygen (O_2 , 99.998%, Matheson), isotopically labeled oxygen ($^{18}O_2$, 95–98% isotopic purity, Cambridge Isotope Labs), nitric oxide (NO, 99.0% minimum purity, Matheson), and isotopically labeled nitric oxide (^{15}NO , 98% isotopic purity, Cambridge Isotope Labs; $^{15}N^{18}O$, 99.9% ^{15}N , 98.4% ^{18}O , Isotec) were used as received. The 1:1 mixture of ^{14}NO and ^{15}NO was prepared in the stainless steel dosing line and stored in a glass equilibration flask, its composition verified by mass spectrometry. Importantly, no impurities (i.e., N_2 , N_2O , NO_2) were detected in the NO samples.

Preparation and characterization of the oxygen overlayers used in this study have been outlined in detail previously.^{18,19} Saturation of the Mo(110) crystal with O_2 at ~ 100 K, followed by heating to 500 K, results in a surface overlayer of oxygen predominantly in low-symmetry, high-coordination sites.¹² The coverage of this overlayer is ~ 0.75 ML, determined by comparison of the O(KLL)/Mo(LMM) Auger ratio with that of a surface of known (0.35 ML) oxygen coverage.²⁰ The same protocol with a lower O_2 exposure generates a 0.4-ML overlayer of oxygen in bridging sites.^{12,19} A thin-film oxide is prepared by exposing the crystal to $\sim 1 \times 10^{-9}$ Torr O_2 for 5 min at 1200 K, cooling the sample to ~ 450 K in the presence of oxygen; this preparation populates the same high coordination sites described above, as well as terminal (Mo=O) sites, and deposits oxygen in the subsurface region as well.^{12,19} X-ray photoelectron studies²¹ give a coverage of $\theta_O \approx 1.7$ ML for a similarly prepared surface; Auger electron spectroscopy gives a value of $\theta_O \approx 1$ ML.

Results

Temperature Programmed Reaction. Nitric oxide dissociation is inhibited by the presence of oxygen chemisorbed in high-coordination sites. Dissociation is the major reaction pathway for NO reaction on clean Mo(110) and is detected by recombinant formation of dinitrogen (N_2) at ~ 1200 K. On an oxygen overlayer comprised of ~ 0.4 ML of chemisorbed oxygen in bridging sites,²² the amount of recombinant N_2 produced from reaction of a saturation dose of NO (Figure 1b) is approximately 3 times less than on clean Mo(110) (Figure 1a). An increase

TABLE 1: Relative Yields of Products from NO Reaction on Clean and Oxygen-modified Mo(110)^a

θ_O	N_2O	N_2 (low-T)	NO	N_2 (~ 1200 K)	total amount of reaction
0 ML	0.13	0.11	0.03	0.73	1
0.75 ML	0.35	0.28	0.23	0.14	0.23
>1 ML	0.29	0.25	0.46	0	0.36

^a Yields of individual products are expressed as percentages of the total reaction for that surface. The amount of total reaction on each surface is normalized to 1 on clean Mo(110).

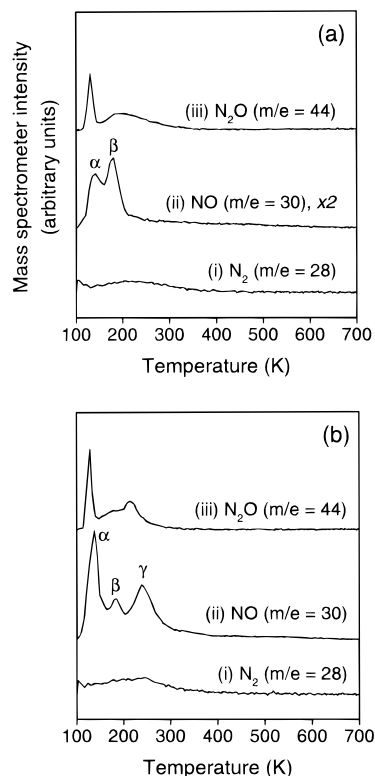


Figure 2. Temperature programmed reaction of a saturation coverage of NO at ~ 100 K on (a) 0.75-ML oxygen overlayer on Mo(110) and (b) thin-film oxide on Mo(110). Products are (i) N_2 , (ii) NO, and (iii) N_2O . Both $m/e = 30$ and $m/e = 28$ have been corrected for cracking from N_2O . Vertical scales are identical in (a) and (b); note magnified scale for $m/e = 30$ in (a). The heating rate was nonlinear but highly reproducible and varied from ~ 20 – 5 K s^{-1} over the range from ~ 100 to 750 K.

in θ_O from 0.4 to 0.75 ML results in an additional 5-fold decrease in the amount of NO dissociation (Figure 1c). On the thin-film oxide, virtually no NO dissociation is detected (Figure 1d).

As on clean Mo(110), both reactions proceeding via N–N bond formation to evolve N_2 and N_2O and molecular desorption of NO are observed below 600 K on oxygen-modified surfaces. The relative amounts of products observed from reaction of NO on the oxygen-modified surfaces are compared with clean-surface products in Table 1. On the 0.75-ML oxygen overlayer, N_2O formation accounts for the majority of this low-temperature reaction, and indeed the majority of total NO reaction (Figure 2a(curve iii)).²³ The sharp peak in N_2O evolution at ~ 130 K is desorption limited and therefore arises from N_2O formed upon NO adsorption at 100 K; reaction-limited N_2O evolution is complete by ~ 375 K. NO desorption occurs in two distinct peaks, at ~ 140 (α) and ~ 180 K (β), with a long tail to ~ 600 K (Figure 2a(curve ii)). Dinitrogen is evolved in a broad peak below 400 K (Figure 2a.i).

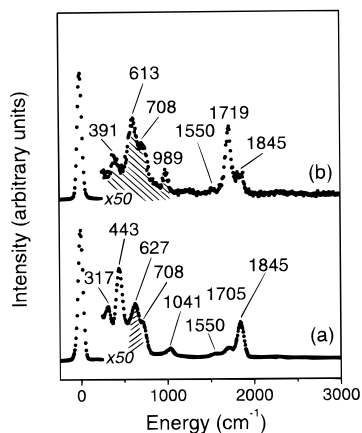


Figure 3. Electron energy loss spectra of saturated NO overlayer at 100 K on (a) 0.75-ML oxygen overlayer and (b) thin-film oxide. Shaded regions correspond to intensity from the oxygen overlayers. Resolution is 65 and 60 cm^{-1} , respectively.

Molecular desorption of NO is the dominant pathway for NO reaction on the thin-film oxide, accounting for almost half the total reaction on that surface (Figure 2b). Three distinct desorption states are observed at 140 (α), 185 (β), and 240 K (γ) (Figure 2b(curve ii)). The same desorption-limited peak in N_2O evolution is observed at ~ 130 K, with reaction to form N_2O complete by ~ 325 K (Figure 2b(curve iii)), approximately 50 K lower than on the 0.75-ML overlayer. A new peak maximum for N_2O evolution is resolved on the thin-film oxide, at ~ 215 K; this same peak is observed after N_2O adsorption on the oxide overlayer and therefore represents a second desorption-limited state. Dinitrogen evolution is similar to that observed on the 0.75-ML overlayer (Figure 2b(curve i)).

No incorporation of surface oxygen into NO or N_2O is observed for NO reaction on either oxygen-modified Mo(110) surface. Specifically, neither N^{18}O nor N_2^{18}O are detected from reaction of NO on an ^{18}O -labeled 0.75-ML overlayer or thin-film oxide. Furthermore, no NO_2 production is detected on any oxygen-modified Mo(110) surface studied.

Electron Energy Loss Spectroscopy. The electron energy loss spectra of NO adsorbed on oxygen-modified Mo(110) reveal several different intact NO species at 100 K, as evidenced by multiple $\nu(\text{NO})$ features (Figure 3). Four distinct $\nu(\text{NO})$ peaks are resolved after adsorption of a saturation dose of NO on the 0.75-ML oxygen overlayer, at 1041, 1550, 1705, and 1845 cm^{-1} (Figure 3a). This is in contrast to the relatively simple electron energy loss spectrum of NO adsorbed on clean Mo(110), for which only two $\nu(\text{NO})$ peaks are observed, at 1726 and 1815 cm^{-1} .⁸

The peak at 1041 cm^{-1} is outside the frequency range normally observed for NO on metal surfaces but shifts as predicted by the harmonic oscillator approximation in isotopic labeling experiments. One possible origin of such a low $\nu(\text{NO})$ frequency is parallel or near-parallel adsorption of NO, resulting in substantial weakening of the N–O bond. Such a species is proposed to give rise to $\nu(\text{NO})$ at 920 cm^{-1} on Rh(100).²⁴ However, parallel NO adsorption should be favored at lower coverages, where access to the surface is less sterically hindered, as observed for parallel-bound NO on Rh(100);²⁴ in the present case, the 1041 cm^{-1} feature is only observed at NO coverages near saturation.

We propose that the most plausible origin of this feature is a surface bound cis-hyponitrite species $(\text{NO})_2^{2-}$, with $\nu_s(\text{NO})$ at 1047 cm^{-1} in NaN_2O_2 .²⁵ A $\nu(\text{NO})$ peak at 1150 cm^{-1} was tentatively assigned to such a species on Ru(001)²⁶ of such a

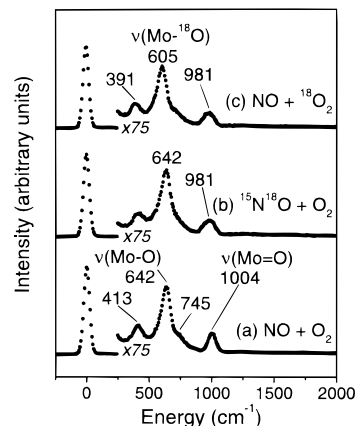


Figure 4. Electron energy loss spectra of atomic oxygen deposited by NO dissociation on 0.75-ML oxygen overlayer after reaction of (a) $^{14}\text{N}^{16}\text{O}$ on an unlabeled oxygen overlayer, (b) $^{15}\text{N}^{18}\text{O}$ on unlabeled oxygen overlayer, and (c) unlabeled NO on ^{18}O -labeled overlayer. In each case a saturated NO overlayer was heated to 600 K. Resolution was 53–55 cm^{-1} in all cases.

species. Formation of nitrite or nitrate (NO_3^-) species, as observed on oxide surfaces,²⁷ is ruled out by the absence of any shift in the 1041 cm^{-1} peak upon ^{18}O labeling of the oxygen overlayer.

The peaks below 800 cm^{-1} in the electron energy loss spectrum of NO on the 0.75-ML overlayer can be assigned to Mo–NO features, with the exception of $\nu(\text{Mo–O})$ from the overlayer at 627 cm^{-1} . From coverage-dependent studies of the electron energy loss spectrum, the peaks at 443 and 708 cm^{-1} appear to be associated with $\nu(\text{NO})$ at 1845 cm^{-1} and are therefore attributed to $\nu(\text{Mo–NO})$ and $\delta(\text{Mo–NO})$, respectively, of that species. The peak at 317 cm^{-1} is assigned to $\nu(\text{Mo–NO})$ of another intact NO species, since it cannot be assigned to any known Mo–O or Mo–N modes.

Adsorption of NO on the thin-film oxide gives rise to three $\nu(\text{NO})$ peaks, at 1550, 1719, and 1845 cm^{-1} (Figure 3b). Whereas the peak at 1845 cm^{-1} is the most intense in the electron energy loss spectrum of NO on the 0.75-ML overlayer, on the thin-film oxide the spectrum is dominated by $\nu(\text{NO})$ at 1719 cm^{-1} . No $\nu(\text{NO})$ features are observed below 1550 cm^{-1} on this surface; the peak at 989 cm^{-1} arises from $\nu(\text{Mo=O})$ of the oxide film.

Electron energy loss spectra of the atomic species left after NO dissociation on the 0.75-ML overlayer (Figure 4) show that NO not only deposits oxygen in terminal (Mo=O) sites, as was observed from NO dissociation on clean Mo(110),⁸ but also displaces surface oxygen from high coordination sites onto terminal sites. After heating NO on the 0.75-ML overlayer to 600 K, the electron energy loss spectrum shows population of high coordination sites ($\nu(\text{Mo–O})$ at 642 cm^{-1} , $\delta(\text{Mo–O})$ at 413 cm^{-1}) and terminal sites ($\nu(\text{Mo=O})$ at 1004 cm^{-1}), as well as oxygen migration into the subsurface region, indicated by the peak at 745 cm^{-1} (Figure 4a).¹² After dissociation of $^{15}\text{N}^{18}\text{O}$ on an unlabeled oxygen overlayer, $\nu(\text{Mo=O})$ has broadened and shifted to 981 cm^{-1} (Figure 4b); the same effect is observed after dissociation of unlabeled NO on an ^{18}O -labeled overlayer (Figure 4c). These peaks are well fit²⁸ by two overlapping peaks, of approximately equal intensity, at 955 and 1004 cm^{-1} . The peak at 955 cm^{-1} corresponds well with $\nu(\text{Mo=}^{18}\text{O})$ observed at 957 cm^{-1} from dissociation of $^{15}\text{N}^{18}\text{O}$ on clean Mo(110).⁸ The broadening of $\nu(\text{Mo=O})$ for isotopically mixed overlayers is not due to ^{16}O contamination in either the labeled NO or oxygen, since dissociation of $^{15}\text{N}^{18}\text{O}$ on an ^{18}O -labeled

feature on the 0.75-ML oxygen overlayer to monomeric NO which reacts in part to form N_2 below 400 K (Figure 2a(curve i)).

The remaining features in the infrared spectrum of NO on the 0.75-ML oxygen overlayer on Mo(110) at 100 K must either dissociate at higher temperatures or contribute to the broad background of NO desorption underlying the two distinct desorption states. The peak observed at 1041 cm^{-1} with electron energy loss spectroscopy is observed as a very small peak at 1033 cm^{-1} in the infrared spectrum (Figure 5a) and is not observed at lower NO coverages, consistent with the formation of a hyponitrite species at high coverages. Unfortunately, the low intensity of this feature precludes definitive identification of such a coupled species via infrared spectroscopy of an isotopically mixed overlayer. The mode detected at 1550 cm^{-1} with electron energy loss spectroscopy (Figure 3a) is assumed to correspond to a species with a low dynamic dipole, since intensity in that region of the infrared spectrum is only detected in a weak, broad peak after annealing to 150 K (Figure 5b).

Correlation of $\nu(\text{NO})$ infrared peaks with NO desorption states from NO adsorption on the thin-film oxide is also straightforward (Figure 6). A peak at 1868 cm^{-1} , present after NO adsorption at 100 K (Figure 6a), disappears upon heating to 180 K (Figure 6b) and is therefore assigned to NO species desorbing in the α state at 140 K (Figure 2b(ii)). The N—O stretch at 1728 cm^{-1} (Figure 6a) sharpens and shifts to 1731 cm^{-1} at 180 K (Figure 6b), then attenuates severely upon heating to 230 K (Figure 6c). While there remains a broad peak at $\sim 1727\text{ cm}^{-1}$ at 300 K, this peak appears to be analogous to the $\nu(\text{NO})$ feature which persists at 1726 cm^{-1} after heating NO on the 0.75-ML overlayer to 300 K (Figure 5d) and is distinct from the sharper peak at 1731 cm^{-1} . Therefore, the peak at 1731 cm^{-1} is assigned to NO which desorbs in the γ state centered at 240 K (Figure 2b(ii)). This assignment is consistent with coverage-dependent infrared spectra in which the appearance of a sharp, narrow $\nu(\text{NO})$ feature at this frequency corresponds with the onset of γ -NO desorption. The smaller β -NO desorption state at $\sim 180\text{ K}$ is associated with the feature at 1558 cm^{-1} (Figure 6a) that is also observed in electron energy loss spectroscopy ($\sim 1550\text{ cm}^{-1}$, Figure 3b).

Dinitrosyls remain on the thin-film oxide even after heating to 300 K, as evidenced by the persistence of $\nu_s(\text{NO})$ at 1822 cm^{-1} (Figure 6d). In fact, this peak is observed even after heating as high as 500 K on both the 0.75-ML overlayer and the thin-film oxide, indicating that the stabilities of these species are relatively invariant with oxygen coverage.

Adsorption of NO on both the 0.75-ML oxygen overlayer on the thin-film oxide prepared with $^{18}\text{O}_2$ shows that none of the $\nu(\text{NO})$ features observed in either the infrared or electron energy loss spectra involve contributions from surface oxygen, since no shift is observed in any of these modes. This is consistent with the lack of incorporation of surface oxygen into any oxygen-containing products evolved from NO reaction on these surfaces.

Discussion

Preadsorption of atomic oxygen on Mo(110) has two main effects on the reactivity of nitric oxide: inhibition of NO dissociation and increasing the favorability of NO desorption over N—N bond formation at low temperature. Since N—N bond formation to evolve N_2 and $N_2\text{O}$ entails deposition of atomic oxygen, the decrease in both the relative and absolute amounts of these products is almost certainly related to the decreased facility of the Mo(110) surface for NO dissociation

in the presence of surface oxygen. This decrease may be due to electronic effects, wherein the electronegative oxygen atoms withdraw electron density from the surface, thereby reducing population of the NO 2π antibonding orbital by metal d electrons and hence strengthening (or reducing surface-induced weakening of) the N—O bond. Such effects have been implicated in the adsorption of NO on oxygen-covered Ni(111), where coadsorption of oxygen and NO actually increased the N—O stretch frequency to a value higher than that of gas-phase NO, suggesting that the charge flow typically associated with π -back-bonding in NO was reversed to depopulate the $2\pi^*$ orbital relative to its gas-phase population of one electron.²⁹

Another mechanism for inhibiting NO dissociation is simple site-blocking by surface oxygen of the sites required for deposition of atomic nitrogen and oxygen from NO. Our electron energy loss spectra do not reveal the preferred binding site for nitrogen upon NO dissociation, since Mo—N features are apparently eclipsed by the more intense Mo—O peaks. On clean Mo(110) oxygen from NO dissociation populates first bridging sites and then a combination of lower symmetry, high-coordination sites and terminal sites.⁸ In the present study, on an oxygen overlayer of $\theta_{\text{O}} \approx 0.4\text{ ML}$ dissociation of NO was decreased to approximately 30% of that on the clean surface. Since oxygen in the $\sim 0.4\text{-ML}$ overlayer resides almost exclusively in long-bridge sites,^{12,18} the sites favored for oxygen deposition in the early stages of NO dissociation on Mo(110), some of the observed decrease in NO dissociation may in fact be due to site blocking. However, the relative importance of the two effects (steric and electronic) cannot be determined without some probe of the change in surface and/or NO electronic structure.

Displacement of surface oxygen from high-coordination to terminal sites by NO dissociation on the 0.75-ML overlayer indicates that, even at a relatively high coverage of oxygen, the driving force for NO dissociation is quite strong. The thermal evolution of thin-film oxides on Mo(110) suggests that highly coordinated oxygen is more stable than terminal oxygen, since Mo=O species convert to highly coordinated species upon heating to 1400 K.¹⁹ The fact that NO dissociation can displace oxygen from high-coordination sites to form Mo=O species suggests that bonding of atomic nitrogen to the surface may play a role as well. Indeed, population of Mo=O sites by NO dissociation on clean Mo(110), which involves no migration of oxygen from high-coordination sites, must be influenced by the simultaneous creation of surface-bound atomic nitrogen, since Mo=O sites are not populated on Mo(110) by dissociated O_2 in the absence of a significant amount of subsurface oxygen.

As mentioned above, the decrease in the amount of low-temperature N—N bond formation with increasing oxygen coverage is likely due at least in part to the inability of the surface to accommodate the additional atomic oxygen deposited by these reactions. It is also possible that fewer of the intermediates leading to N—N bond formation are formed on the oxygen-modified surfaces as compared to the clean surface. However, the persistence of dinitrosyls well beyond the highest temperature for $N_2\text{O}$ evolution on clean Mo(110)⁸ suggests that population of surface sites byproducts of NO dissociation and reaction inhibits $N_2\text{O}$ evolution from these species. Therefore, adsorption of NO on Mo(110) surfaces with a significant concentration of surface oxygen is expected to inhibit dinitrosyl reaction at lower temperatures. While intensity from $\nu_s(\text{NO})$ of dinitrosyls appears to be lower on the thin-film oxide than on the 0.75-ML overlayer, this difference could easily be due

to changes in the local environment of dinitrosyls on the two surfaces and cannot be used to judge relative populations.

Concomitant with the decrease in N–N bond formation is an increase in both the absolute amount and the peak temperatures for NO desorption. It is likely that this effect, too, is related to the ease of NO dissociation, since NO dissociation which is facile upon adsorption on clean Mo(110) may be inhibited in the presence of sufficient surface oxygen. Therefore, nitrosyls which are never observed on the clean surface or at lower oxygen coverages may remain on the oxygen-modified surfaces studied herein until the barrier for Mo–NO bond scission is overcome. The peak temperature for desorption of these species, then, reflects the energetics of the Mo–NO bond in the case where perturbation of the N–O bond is not sufficient to cause, or sites are not available for, dissociation to atomic nitrogen and oxygen. On clean Mo(110) there is only one peak maximum observed for NO desorption, at ~ 130 K.⁸ The highest peak maximum for NO desorption increases to ~ 180 K (β) for the 0.75-ML overlayer and to ~ 240 K (γ) on the thin-film oxide, with significant NO desorption occurring on the latter surface above room temperature (in addition to the weak desorption tail observed to ~ 600 K on all surfaces studied). While all these NO species are relatively weakly bound, the increase in peak maxima from 130 to 240 K gives an increase in desorption activation energy of 28 kJ mol^{-1} as estimated from a Redhead approximation³⁰ using an attempt frequency of 10^{13} .

Importantly, there is no consistent correlation between N–O bond perturbation upon adsorption, as measured by $\nu(\text{NO})$ of surface-bound nitrosyls, and the strength of the metal–NO interactions as measured by desorption temperature. The amount that the $\nu(\text{NO})$ frequency is lowered from the gas phase $\nu(\text{NO})$ of 1876 cm^{-1} is a measure of how much charge transfer takes place via π -back-bonding from the surface to the 2π antibonding orbital of NO. However, the results presented herein demonstrate that the amount of apparent N–O bond perturbation does not predict the strength of the NO–metal interaction. For instance, on the thin-film oxide, γ -NO, with $\nu(\text{NO})$ of 1731 cm^{-1} , desorbs at a higher temperature than the β -NO, with $\nu(\text{NO})$ of 1558 cm^{-1} . On the 0.75-ML oxygen overlayer, β -NO has an N–O stretch frequency 9 cm^{-1} higher than that of α -NO, which has a peak desorption temperature ~ 40 K higher. One explanation for this phenomenon may be that entropic effects play a large role in determining NO desorption peak temperatures in this system, since the equation of desorption temperature with the strength of the Mo–NO bond assumes an identical attempt frequency for all species. Without detailed structural information about the surface nitrosyls in these systems, it is impossible to evaluate their relative entropies of activation; however, it is important to realize that such effects may play an important part in determining the small observed differences in stability of surface nitrosyls.

There are two general mechanisms by which oxygen might alter Mo–NO bonding. Electronic modification of a clean-surface binding site may allow NO on the oxygen-covered surface to adsorb in the same site, but with altered intramolecular and metal–NO bonding as reflected in $\nu(\text{NO})$. In addition, the presence of surface oxygen may induce NO adsorption at a site not populated on the clean surface, either by electronic stabilization of the new site or by destabilization of the old site via site-blocking and/or electronic effects. Both of these phenomena have been observed previously after NO adsorption on other transition metal surfaces.

A combination of these two effects is observed for NO due to oxygen-modification of Ni(111): an upshift in the frequencies of two nitrosyl species with $\nu(\text{NO})$ near 1500 cm^{-1} as a function of oxygen coverage, and formation of a set of nitrosyl species not observed on clean Ni(111), with frequencies in the range 1800 – 1888 cm^{-1} .²⁹ A similar upshift in $\nu(\text{NO})$ of one nitrosyl species with increasing θ_{O} is observed on Pt(111).³¹ The formation of new nitrosyls species with $\nu(\text{NO})$ frequencies substantially higher than those observed on the corresponding clean surfaces occurs upon oxygen modification of both Rh(111)³² and Ni(100).³³

Although N–O bonds in the nitrosyls described above are apparently strengthened by interactions with coadsorbed oxygen, the thermal stability of these species varies qualitatively among surfaces. On Rh(111),³⁴ Ni(111),³⁵ and Pt(111),³¹ NO exhibits lower desorption temperatures in the presence of oxygen, in contrast to the higher desorption temperatures observed for NO on oxygen-modified Mo(110). However, on Ni(100), as on oxygen-modified Mo(110), NO desorption occurs at higher temperatures in the presence of oxygen, again suggesting that the effect of oxygen coadsorption on the metal–NO bond cannot be directly inferred from the extent of metal–NO interaction indicated by perturbation of the N–O stretch frequency.

The modification of NO species by preadsorbed oxygen on Mo(110) is slightly more complex than in the systems discussed above, since $\nu(\text{NO})$ frequencies both higher and lower than on clean Mo(110)⁸ are observed from NO adsorption on the oxygen-modified surfaces. This qualitative variation in the effect of oxygen on N–O bond strength indicates that NO bonding to Mo(110) is strongly dependent on local electronic structure rather than on the overall extent of surface oxidation. At this time, the structural details of these oxygen overlayers on Mo(110), and hence the bonding environments available to NO on these surfaces, are not well understood; combined LEED and STM experiments in our laboratory seek to address this problem.

Although preadsorption of surface oxygen has a significant effect on the mononitrosyl species observed on Mo(110), it seems to have no dramatic effect on dinitrosyls. This is surely related to the fact that dinitrosyl formation on the “clean” Mo(110) surface does not occur until dissociation of a significant amount of NO has deposited ~ 0.5 ML of atomic oxygen on that surface.⁸ Dinitrosyls are observed at the same maximum temperature (~ 500 K) on both the clean and oxygen-modified surfaces, with no detectable change in the frequency for $\nu_s(\text{NO})$. This suggests that dinitrosyls will only form at a very specific site, since presumably Mo atoms with very different oxidation states are available on the oxygen overlayer and thin-film oxide. The fact that dinitrosyls do not form on clean Mo(110) until substantial NO dissociation has occurred suggests that they require a site modified by oxygen, but the exact nature of that site is unknown at this time. It seems likely, however, by comparison with dichlorodinitrosylmolybdenum,³⁶ that dinitrosyls form at an atop site rather than bridging multiple Mo atoms. Electronic structure calculations are currently underway in our laboratory to address this point via an understanding of dinitrosyl bonding to MoO_3 .

The complexity of the vibrational spectra of NO overlayers on oxygen-modified Mo(110) underscores the necessity of examining such systems with the higher resolution of infrared spectroscopy, since chemically distinct NO species are shown to exhibit such similar $\nu(\text{NO})$ frequencies that they are not resolvable with electron energy loss spectroscopy. In fact a combination of the two techniques is vital to studies such as

this, since the effects of atomic species are best studied with the electron energy loss spectroscopy.

Conclusions

In summary, we have shown that reaction of NO on oxygen-modified Mo(110) surfaces is characterized by a decrease in facility for NO dissociation and a concomitant increase in both the relative and absolute amounts of molecular NO desorption. Formation of N–N bonds from intact molecules to evolve N₂ and N₂O, while occurring to a lesser extent than on the clean surface, results from analogous reaction pathways. This decrease in NO reduction chemistry at low temperatures is proposed to result from the decreased facility for N–O bond scission that inhibits complete NO dissociation, but may also arise from a lower concentration of the relevant species or a combination of these two effects.

New NO desorption features are observed both on the 0.75-ML oxygen overlayer and on the thin-film oxide and are correlated with distinct NO species (identified by $\nu(\text{NO})$ frequency). While there is evidence for strengthening of the N–O bond in some of these species, indicated by increased $\nu(\text{NO})$ frequencies relative to those observed on the clean surface, in some cases the oxygen-dependent species exhibit vibrational frequencies lower than those observed from NO adsorption on clean Mo(110). As has been suggested from results on other transition metal surfaces, metal–NO bond strength may be altered either in concert or in opposition to N–O bond strength by coadsorption of oxygen. Therefore, stability of nitrosyls to both desorption and dissociation is proposed to be very sensitive to the local environment and cannot be easily explained by overall changes in the surface electron density.

Acknowledgment. The authors gratefully acknowledge support of this work by the U. S. Department of Energy, Office of Basic Energy Sciences, under Grant DE-FG02-84-ER13289.

Supporting Information Available: Infrared spectra of dinitrosyls in isotopically mixed NO overlayers on both the 0.75-ML oxygen overlayer and the thin-film oxide on Mo(110) (2 pages). Ordering information is given on any current masthead page.

References and Notes

- (1) Yao, H. C.; Rothschild, W. G.; Gandhi, H. S. *Stud. Surf. Sci. Catal.* **1984**, *19*, 71–75.
- (2) Halasz, I.; Brenner, A.; Shelef, M. *Catal. Lett.* **1992**, *16*, 311–321.
- (3) Halasz, I.; Brenner, A.; Shelef, M. *Catal. Lett.* **1993**, *18*, 289–297.
- (4) Halasz, I.; Brenner, A.; Shelef, M. *Catal. Lett.* **1993**, *22*, 147–156.
- (5) Kazusaka, A.; Howe, R. F. *J. Catal.* **1980**, *63*, 447–455.
- (6) Millman, W. S.; Hall, W. K. *J. Phys. Chem.* **1979**, *83*, 427–428.
- (7) Yao, H. C.; Rothschild, W. G. Surface interaction in the MoO₃/γ-Al₂O₃ system. II. Effect of surface structure on NO chemisorption. *Proceedings of the International Conference of the Chemistry and Uses of Molybdenum*; 1982. Ann Arbor: MI.
- (8) Queeney, K. T.; Friend, C. M. *J. Chem. Phys.* **1997**, *107*, 6432–6442.
- (9) Brown, W. A.; Gardner, P.; King, D. A. *J. Phys. Chem.* **1995**, *99*, 7065–7074.
- (10) Brown, W. A.; Gardner, P.; Perez Jigato, M.; King, D. A. *J. Chem. Phys.* **1995**, *102*, 7277–7230.
- (11) Dumas, P.; Suhren, M.; Chabal, Y. J.; Hirschmugl, C. J.; Williams, G. P. *Surf. Sci.* **1997**, *371*, 200–212.
- (12) Colaianni, M. L.; Chen, J. G.; Weinberg, W. H.; Yates, J. T. *Surf. Sci.* **1992**, *279*, 211–222.
- (13) Wiegand, B. C.; Uvdal, P. E.; Serafin, J. G.; Friend, C. M. *J. Am. Chem. Soc.* **1991**, *113*, 3(17), 6686–6687.
- (14) Weldon, M. K.; Friend, C. M. *Surf. Sci.* **1994**, *310*, 95–102.
- (15) Liu, A. C.; Friend, C. M. *Rev. Sci. Instrum.* **1986**, *57*, 1519–1522.
- (16) Roberts, J. T.; Friend, C. M. *J. Am. Chem. Soc.* **1986**, *108*, 7204–7210.
- (17) While infrared spectra were collected at 4 cm^{−1} in order to minimize drift in water background, improving the resolution to 2 cm^{−1} did not resolve any new features.
- (18) Queeney, K. T.; Friend, C. M. *J. Chem. Phys.* **1998**, *109*, 6067–6074.
- (19) Queeney, K. T.; Friend, C. M. *J. Phys. Chem. B* **1998**, *102*, 5178–5181.
- (20) Chen, D. A.; Friend, C. M. *J. Phys. Chem.* **1997**, *101*, 5712–5716.
- (21) Chen, D. A.; Friend, C. M. *J. Am. Chem. Soc.* **1998**, *120*, 5017–5023.
- (22) This overlayer was prepared with the same protocol as that used for the 0.75-ML overlayer, with a smaller dose of O₂. Electron energy loss spectroscopy demonstrates that oxygen occupies exclusively bridging sites ($\nu(\text{Mo–O}) = 546 \text{ cm}^{-1}$) at this coverage.^{12, 37}
- (23) “Total reaction” is used herein to denote NO molecular desorption as well as N₂O and N₂ production and dissociation, to provide some measure of the activity of these surfaces for NO reduction.
- (24) Villarubia, J. S.; Richter, L. J.; Gurney, B. A.; Ho, W. J. *Vac. Sci. Technol. A* **1986**, *4*, 1487–1490.
- (25) Laane, J.; Ohlsen, J. R. *Prog. Inorg. Chem.* **1980**, *27*, 465–513.
- (26) Thiel, P. A.; Weinber, W. H.; Yates, J. T., Jr. *Chem. Phys. Lett.* **1979**, *67*, 403–407.
- (27) Busca, G.; Lorenzelli, V. J. *Catal.* **1981**, *72*, 303–313.
- (28) The peaks were fit with Gaussian line shapes of the same or greater width (fwhm) as the elastic peak in the corresponding spectrum.
- (29) Chen, J. G.; Erley, W.; Ibach, H. *Surf. Sci.* **1989**, *224*, 215–234.
- (30) Redhead, P. A. *Vacuum* **1962**, *12*, 203–211.
- (31) Bartram, M. E.; Koel, B. E.; Carter, E. A. *Surf. Sci.* **1989**, *219*, 467–489.
- (32) Root, T. W.; Fisher, G. B.; Schmidt, L. D. *J. Chem. Phys.* **1986**, *85*, 4687–4695.
- (33) Odorfer, G.; Jaeger, R.; Illing, G.; Kühlenbeck, H.; Freund, H.-J. *Surf. Sci.* **1990**, *233*, 44–58.
- (34) Root, T. W.; Schmidt, L. D.; Fisher, G. B. *Surf. Sci.* **1983**, *134*, 30–45.
- (35) Bozso, F.; Arias, J.; Hanrahan, C. P.; Yates, J. T.; Martin, R. M.; Metiu, H. *Surf. Sci.* **1984**, *141*, 591–603.
- (36) Cotton, F. A.; Johnson, B. F. G. *Inorg. Chem.* **1964**, *3*, 1609–1612.
- (37) Queeney, K. T. Ph.D. Thesis, Harvard University, 1998.